Performance enhancement of GaN metal–semiconductor–metal ultraviolet photodetectors by insertion of ultrathin interfacial HfO$_2$ layer

Manoj Kumar, Burak Tekcan, and Ali Kemal Okyay

Performance enhancement of GaN metal–semiconductor–metal ultraviolet photodetectors by insertion of ultrathin interfacial HfO₂ layer

Manoj Kumar[a)]
UNAM-National Nanotechnology Research Center and Institute of Materials Science and Nanotechnology, Bilkent University, 06800 Ankara, Turkey

Burak Tekcan and Ali Kemal Okyay[a)]
UNAM-National Nanotechnology Research Center and Institute of Materials Science and Nanotechnology, Bilkent University, 06800 Ankara, Turkey and Department of Electrical and Electronics Engineering, Bilkent University, 06800 Ankara, Turkey

The authors demonstrate improved device performance of GaN metal–semiconductor–metal ultraviolet (UV) photodetectors (PDs) by ultrathin HfO_2 (UT-HfO_2) layer on GaN. The UT-HfO_2 interfacial layer is grown by atomic layer deposition. The dark current of the PDs with UT-HfO_2 is significantly reduced by more than two orders of magnitude compared to those without HfO_2 insertion. The photoresponsivity at 360 nm is as high as 1.42 A/W biased at 5 V. An excellent improvement in the performance of the devices is ascribed to allowed electron injection through UT-HfO_2 on GaN interface under UV illumination, resulting in the photocurrent gain with fast response time. © 2015 American Vacuum Society. [http://dx.doi.org/10.1116/1.4905735]

I. INTRODUCTION

Owing to direct wide band gap, high saturation velocity and excellent thermal and chemical stability, GaN is considered one of the most promising semiconductor materials for ultraviolet (UV) photodetector (PD) application fields such as flame detectors, space to space detection and solar UV monitoring.[1–3] Various types of UV PD structures based on GaN are examined and among them metal–semiconductor–metal (MSM) PD is a promising candidate due to its easy fabrication and compatibility with field effect transistor based electronics.[4–8] However, the performances of GaN based PDs are still not up to the expectation, due to the excessive leakage current because of high dislocation densities that exist in the GaN thin films. Several developments such as AlGaN/GaN metal-insulator-semiconductor PDs, AlGaN on Si inverted Schottky PDs and inverted AlGaN/GaN UV p-i-n PDs are demonstrated in this direction but most of them suffered from performance limitation especially low photoresponsivity.[9–11] To facilitate further progress, it is vital to develop high responsivity PDs with inherent gain for detecting very low level light signal. Although, MSM PDs can exhibit internal gain that provides high responsivity, it is a slow process. Furthermore, the observed gain in GaN based MSM PDs is mainly caused by dislocation defects in the GaN thin films and existence of trapping states at the semiconductor and metal interface and are generally accompanied by large dark current and long response time. The utilization of interfacial insulating layer is an effective approach to suppress the leakage current and improve the device performance. Sang *et al.*[12] have proposed to utilize CaF_2 as an insulation layer to reduce dark current on InGaN and succeeded to suppress dark current by 6 orders of magnitude in comparison to without CaF_2. Lee *et al.*[13] have

suppressed dark current of GaN based UV PDs by depositing GaO_x in between metal and the GaN. Various insulating materials such as SiO_2, ZrO_2, and Al_2O_3 are reported.[14–16] However, low dielectric constant (k) value restricts the maximum permissible electric field to the device. Therefore, high-k insulating material is helpful in reducing the field strength within the dielectric and thus allowing better performance of the devices. Moreover, it is essential for behaving perfect insulator on GaN, high k material band off set should exceed 1 eV and recent studies reveal that the interfacial layers also play an important role.[17] HfO_2 is a suitable high-k material which has recently gained significant attention. In the present study, atomic layer deposition (ALD) grown UT-HfO_2 layer is inserted between metal and underlying GaN. The thickness of the HfO_2 layer is chosen as 1.5 nm so as not to produce any adverse effect on photocurrent. The dark current is observed to reduce more than 2 orders of magnitude and improved photo-to-dark current contrast ratio, and higher responsivity with internal gain. The dark and photocurrent studies are discussed in terms of carrier transport mechanism at the interface.

II. EXPERIMENT

The GaN samples used in this work were commercially available and grown using metal organic chemical vapor deposition technique on sapphire. The epilayer consisted of 1.2 μm Si doped GaN and 300 nm unintentionally doped GaN. The nominal Hall Effect measured carrier concentration was found to be 1.4×10^{18} and 1.1×10^{17} cm^{-3}, respectively. GaN samples were cleaned using acetone and isopropyl alcohol and then unintentionally grown oxide layer was etched by buffered hydrofluoric acid. Then, the insulating layer UT-HfO_2 was deposited on top of the GaN in Ultratech/Cambridge Nanotech Savannah 100 ALD system with tetrakis (dimethylamido) hafnium and H_2O as

a)Authors to whom correspondence should be addressed; electronic addresses: panwarm72@yahoo.com; aokyay@ee.bilkent.edu.tr

precursors. The base pressure was maintained at 1 Torr during deposition.

Magnetron sputtered 10/100 nm thick Ni/Au interdigitated fingers (rectangular shaped of 5×110 μm with spacing of 10 μm) were directly fabricated on GaN. 10/100 nm thick Ni/Au and 100 nm thick Ni fingers were deposited on two batches of UT-HfO$_2$/GaN samples. The deposition was carried out in a vacuum chamber evacuated at base pressure of 5.6×10^{-6} Torr. High purity Ar was used as sputtering gas. During the Ni deposition power of 125 W, gas flow rate of 50 sccm, deposition time of 1 min, and pressure of 20 mTorr were kept constant. Au was fabricated at constant power of 75 W, gas flow of 50 sccm and pressure of 1 mTorr.

The current–voltage (I-V) measurements were performed using semiconductor parameter analyzer (Keithley 4200) and Keithley 2400 Sourcemeter. The spectral response was obtained by using a lock-in amplifier (SRS820) with an optical chopper and a monochromator from 300 to 420 nm with a 150 W xenon arc lamp. In order to measure photocurrent time response, a UV light source, a resistor of 100 Ω, and Keithley 2400 Sourcemeter were used.

III. RESULTS AND DISCUSSION

The typical room temperature dark and photo I-V characteristics of GaN MSM UV PDs without and with UT-HfO$_2$ prepared with different metal interdigitated fingers are illustrated in Fig. 1. The optical power of 36.89 μW at 360 nm UV illumination was kept constant during the measurements of photocurrent. It is clearly seen from Fig. 1 that devices with UT-HfO$_2$ interfacial layer dark current is reduced more than 2 orders of magnitude at a bias of 10 V. The Au/Ni/GaN device fabricated without UT-HfO$_2$ insertion exhibited dark current of 1.10×10^{-4} A; however, UT-HfO$_2$ introduced devices with different metal interdigitated fingers, namely, Ni/HfO$_2$/GaN and Au/Ni/HfO$_2$/GaN revealed dark current of 1.26×10^{-6} and 7.9×10^{-7} A, respectively, at a bias of 10 V. This demonstrates that UT-HfO$_2$ layer is an effective insulating layer for GaN based devices. Higher photo-to-dark current contrast ratios were also observed in both UT-HfO$_2$ inserted devices in comparison to without
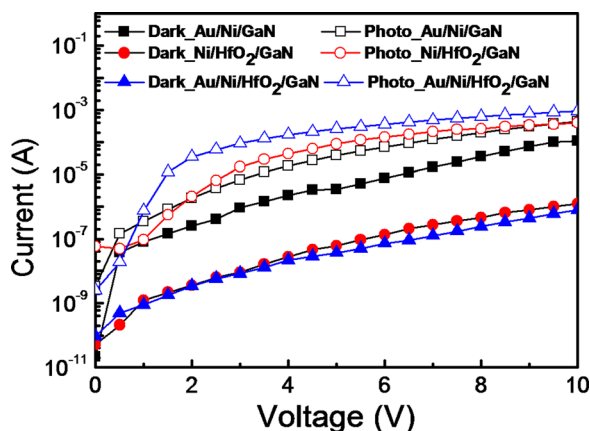
UT-HfO$_2$ inserted device. As can be seen from Fig. 1 that the highest photo-to-dark current contrast ratio is provided by UT-HfO$_2$ inserted device with Au/Ni fingers at bias voltage of 5 V. It is supposed that UT-HfO$_2$ acts to highly suppress the surface defects, resulting in the reduction of recombination centers at the interface. This leads to a reduced dark current due to less thermal generation of carriers and increased photocurrent owing to higher collection efficiency with reduced recombination centers. It is suggested in the literature that introduction of thin insulation layer in-between metal and underlying semiconductor layer drastically reduced dark current and simultaneously decrease photocurrent as well. On the contrary, after insertion of UT-HfO$_2$ layer, photocurrent was found to increase. It is believed that UT-HfO$_2$ layer might have composed of either *coalescence*/island or dense nanoparticle over the GaN, which may scatter the incident light and thus increase the optical absorption and generate more electron-hole pairs. Sun et al.[18] have effectively enhanced optical absorption efficiency after depositing SiO$_2$ nanoparticles on GaN surface. They have also observed that the dense nanoparticles further improved both electrical and optical properties of the GaN MSM UV PDs. Derkacs et al.[19] also utilized SiO$_2$ nanoparticles for improving optical absorption efficiency in GaAs based solar cell.

Figure 2 shows responsivity spectra of GaN based MSM UV PDs without and with UT-HfO$_2$ insertion using different metal interdigitated fingers at a bias voltage of 5 V. All the devices clearly demonstrate relatively flat response at shorter wavelength side and sharp intrinsic transition above the band edge of GaN occurred at 360 nm. The measured peak responsivities of GaN MSM UV PDs without and with UT-HfO$_2$ layer prepared with Au/Ni, Ni, and Au/Ni interdigitated fingers were found to be 0.313, 0.47, and 1.42 A/W, respectively. The measured responsivities of all the devices are larger than the theoretical values ($\sim$0.29 A/W) of a GaN based PD, supporting presence of internal gain in the devices. It is clearly seen from Fig. 1 that the photogenerated current of UT-HfO$_2$ inserted UV PD prepared of Au/Ni interdigitated fingers is higher, thereby obtained the highest

FIG. 1. (Color online) Typical room temperature dark and photo I-V characteristics of without and with UT-HfO$_2$ inserted in between metal and underlying GaN MSM UV PDS prepared with different interdigitated fingers.
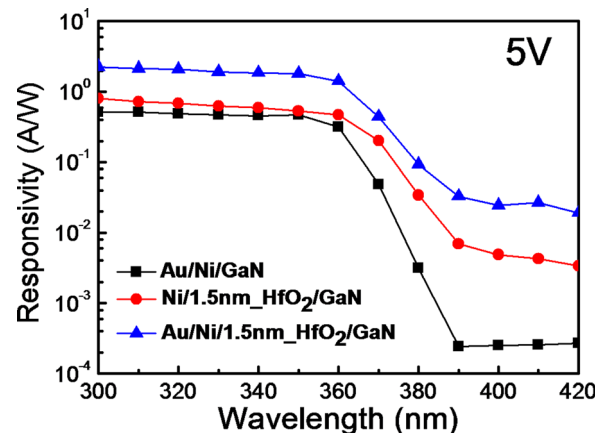

FIG. 2. (Color online) Spectral responsivity of MSM UV PDs fabricated without and with UT-HfO$_2$ inserted in between metal and underlying GaN prepared with different interdigitated fingers.

responsivity among the devices. UV to visible rejection ratio of GaN based MSM UV PDs without UT-HfO$_2$ insertion was obtained to be more than 3 orders of magnitude as defined the responsivity measured at 360 nm divided by that measured at 400 nm. However, it became smaller after introducing UT-HfO$_2$ interfacial layer, which may be due to high densities of defects introduced at the interface.

It is reported in the literature that Ni grows in pseudomorphic form when thickness is less than 10 nm and for higher thicknesses, FCC Ni is formed with many twins and stacking faults. In case of Ni-only metal electrode, Ni thickness was 100 nm. It is believed that FCC Ni is formed along with twins and stacking faults. Due to twins and stacking faults higher trap density exists at Ni/HfO$_2$ interface, which are responsible for electron capture. The captured electrons lead to the formation of a trapped electron charge space. These trapped electrons acts as hole traps and tend to capture photogenerated free holes from the GaN layer. Therefore, this trapping process increases the probability of the recombination of photogenerated carriers at the interface. On the other hand, for 10 nm Ni capped with Au, which not only prevents oxidation, but also improves conductivity of the contact during operation. Hence, Ni/Au metal electrode exhibits much better effect on improving the photocurrent responsivity of devices compared with Ni-only electrode.

Chen et al[20] has reported that the spectral responsivity considerably increased after inserting a thin Si$_3$N$_4$ insulator layer. The significant improvement in responsivity after inserting a thin Si$_3$N$_4$ insulator layer is attributed to the enhancement of the effective surface barrier height and the reduction of the surface recombination loss. Si$_3$N$_4$ can reduce the density of defect states by surface passivation and hence decrease the probability of the surface recombination of photogenerated carriers. However, in the present study, formation of coalescence/island or dense nanoparticles of HfO$_2$ over the GaN layer, which terminate the dislocation defects. Thus, higher responsivity along with internal gain was obtained.

It is assumed that gain larger than theoretical value is related to charge trapping at the interface during illumination. It may be either thermionic field emission or tunneling model played major role for the carrier transportation. The thermionic field emission current density is given by[21]

$$J_{TFE} = J_s \exp\left(\frac{V}{E_0}\right) \left[1 - \exp\left(\frac{-qV}{kT}\right)\right], \quad (1)$$

$$E_0 = E_{00} \coth\left(\frac{E_{00}}{kT}\right), \quad (2)$$

$$E_{00} = \left(\frac{q\hbar}{2}\right)\left(\frac{N_t}{m^* \varepsilon_s}\right)^{1/2}, \quad (3)$$

where q, N_t, m^*, and ε_s are elementary charge, carrier concentration, effective mass, and dielectric constant of the semiconductor, respectively. E_{00} reflects the tunneling probability. In the present case, $m^* = 0.22$ m_0 and $\varepsilon_s = 9.5$ for GaN, and the carrier concentration N_t of the GaN film obtained by Hall measurement is about 1.0×10^{17} cm^{-3}.

The estimated tunneling factor (E_{00}) was found to be 1.15 meV, which is much smaller than the thermal energy k_{BT} at room temperature (26 meV).

In order to investigate further the mechanism of the higher photoresponse phenomenon, the dark and photo I-V characteristic at forward bias were analyzed and the fitted I-V characteristics is shown in Figs. 3(a) and 3(b). It is interesting to note that different carrier transport mechanisms are dominant depending on applied voltage. It is found that Fowler–Nordheim (F-N) tunneling is the dominant conduction mechanism in all the devices at higher applied voltage. The F-N tunneling current is expressed by[22]

$$J_{FN} = V^2 \exp\left(\frac{B}{V} + A\right), \quad (4)$$

where A and B are constants given by $A = q^2/(8\pi h d^2 \phi)$ and $B = 4(\sqrt{2qm^*m_0\phi^{3/2}/3\hbar})$.

In the above equation, ϕ stands for the barrier height in eV, m^* is the effective electron mass, d is the tunnel barrier width, m_0 is the free electron rest mass, Q is the electron charge, and $\hbar$ is the reduced Plank's constant. Figure 4 demonstrates the $\ln(I/V^2)$ vs $1/V$ F-N plot of forward dark and photo I-V characteristics of all the devices. At higher bias
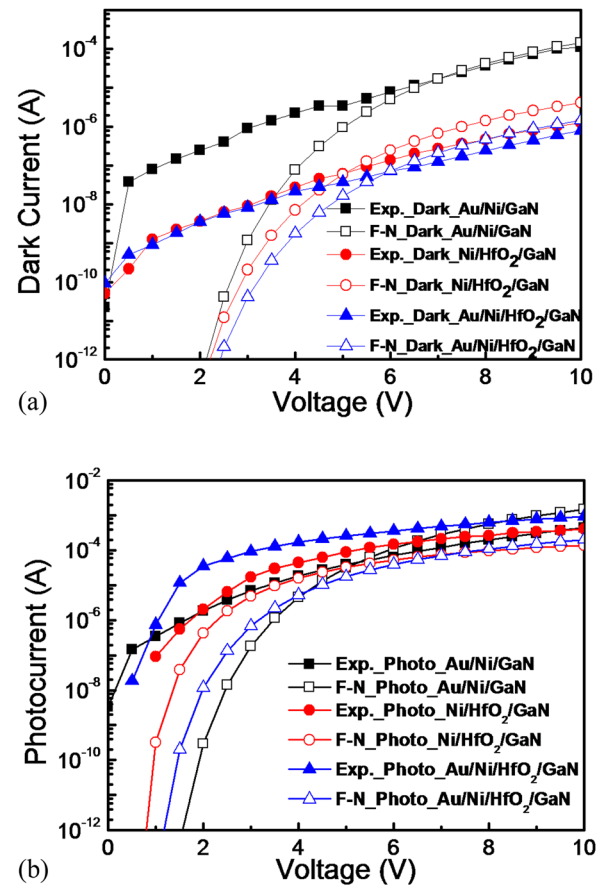

(a)

(b)

FIG. 3. (Color online) Fitting of forward (a) dark and (b) photo I-V characteristics by F-N tunneling of MSM UV PDS fabricated without and with UT-HfO$_2$ inserted in between metal and underlying GaN prepared with interdigitated fingers.
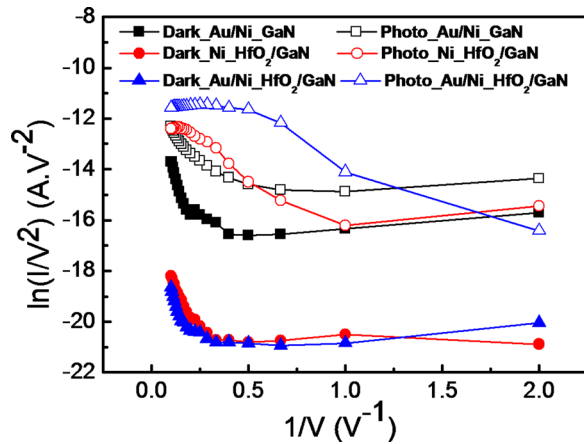
FIG. 4. (Color online) F-N plot of forward dark and photo I-V characteristics of MSM UV PDS fabricated without and with UT-HfO$_2$ inserted in between metal and underlying GaN prepared with different interdigitated fingers.

voltage ln(I/V^2) vs $1/V$ plot is found to linearly decrease having negative slope, which is a characteristics of F-N tunneling model. The F-N tunneling governs the photocurrent at higher applied voltage. It is also confirmed from fitting results that illuminated devices generates additional charge

of acceptor type traps close to the interface. The above analysis suggests that the observed gain is related to charge trapping at the interface during illumination. It can be realized that different carrier transport mechanism is dominated depending on applied voltage. At low bias voltage, the carrier transport is dominated by themionic field emission whereas F-N tunneling is dominated at higher voltage.

The conduction band off set was calculated by F-N tunneling model and the valence band offset was obtained by $E_v = E_{HfO_2} - E_{GaN} - \phi_B$ where E_v, E_{HfO_2}, and E_{GaN} are the valence band offset and the band gap of HfO$_2$ and GaN, respectively.[23] The band diagram of without and with UT-HfO$_2$ devices prepared with different metal fingers are displayed in Fig. 5. The valence band off set value of the dark and illuminated device without UT-HfO$_2$ insertion was calculated as 1.69 and 1.79 eV, respectively. The photogenerated holes drifted toward the cathode are accumulated at the interface due to band bending. These accumulated holes are then captured by the surface states and some of them are trapped at the GaN surface because of existence of dislocation defects at the surface, which behaves as an acceptor like nature.[24] It is assumed that hole trapping causes electron swept out or re-injected in order to maintain charge
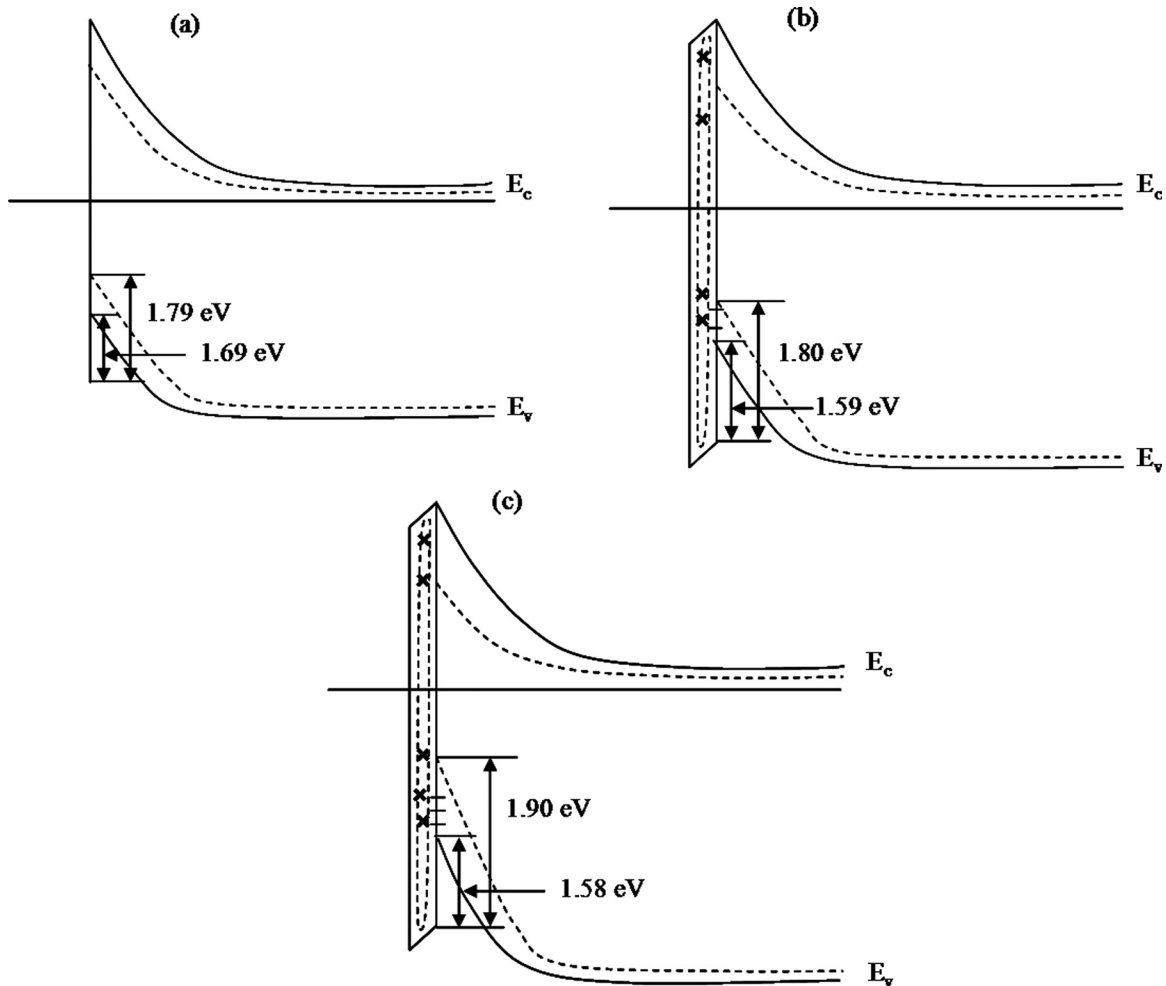

FIG. 5. Qualitative band diagram of (a) without HfO$_2$ inserted MSM UV PD prepared with Au/Ni interdigitated fingers, (b) with HfO$_2$ inserted MSM UV PD fabricated with Ni interdigitated fingers, and (c) with HfO$_2$ inserted MSM UV PD fabricated with Au/Ni interdigitated fingers.

neutrality in the space charge region. This action is responsible for observed gain in the device. The calculated valence band offsets of the devices inserted with UT-HfO$_2$ and prepared with Ni and Au/Ni metal fingers are obtained as 1.80 and 1.90 eV, respectively, which is higher than that of without UT-HfO$_2$ inserted device. The UT-HfO$_2$ inserted device prepared with Au/Ni finger exhibited maximum valence band offset, leading larger number of holes to accumulate and get trapped at the interface and produces the highest responsivity with internal gain. It is widely recognized that the occurrence of gain in the GaN based devices is associated with longer life-time of photogenerated holes.[25] The longer life-time of holes is usually induced by trapping either at interface or on the surface of the active layer. Interface states occur during device formation. It is justified that the occurrence of gain in the present study is due to hole trapping, resulting in electrons being swept out rapidly and circulating many times through external circuit before recombining with holes. It is observed that gain appeared in the device fabricated without UT-HfO$_2$ accompanied by a slow time response as shown in inset of Fig. 6; on the other hand, the devices prepared with UT-HfO$_2$ revealed fast time response despite higher gain. The obtained high response speed might be due to relative shallow energy level of trapped holes. Deeper traps have longer charge release time and thus result in a slower device response. It is mentioned in the literature that the PD response speed is related to the trap occupancy, which depends on light intensity. At low intensity, the photocurrent decay is expected to be dominated by the slower process, because deeper traps are easier to be field. Time response was also measured with low (10 μW) and high power intensity (36 μW) and the device without UT-HfO$_2$ interfacial layer revealed slow response however, UT-HfO$_2$ inserted devices exhibited fast responses with low and high power intensity (low power intensity data are shown here). The assurance of fast response of UT-HfO$_2$ inserted devices with low and high power intensity suggests that either tiny or no deep traps are generated by introducing UT-HfO$_2$ layer.

These features denote that UT-HfO$_2$ plays crucial role in controlling the photoresponse of the GaN MSM UV PDs and

it performs an effective insulation in the dark condition, which reduces the influence of dislocation defects and suppress the dark current. Furthermore, it enhanced light absorption on the active layer, thereby device performance improved. The measurements were also repeated at a certain time interval to test the reproducibility of the devices and every time similar results were obtained.

IV. CONCLUSION

In conclusion, we have investigated dark and photocurrent characteristics of without and with UT-HfO$_2$ inserted GaN UV PDs. Introducing UT-HfO$_2$ interfacial layer reduced dark current more than two orders of magnitude and increased the photocurrent. The device prepared with Au/Ni fingers on UT-HfO$_2$ inserted GaN UV PD exhibit the highest responsivity of 1.42 A/W at wavelength of 360 nm and applied bias of 5 V. The UT-HfO$_2$ inserted devices maintained fast response time in spite of showing gain. The present results demonstrate that UT-HfO$_2$ is a potential candidate for insulation of GaN based UV PDs and optoelectronic devices.
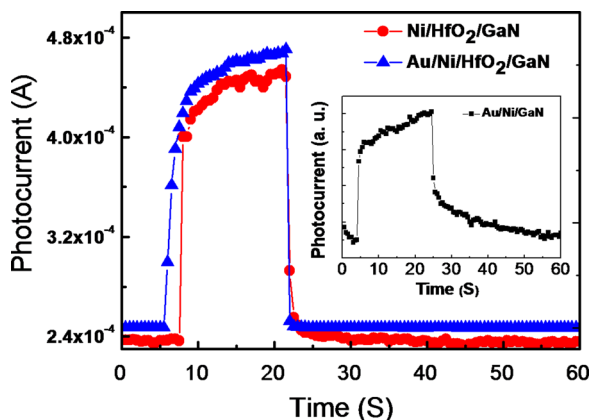
FIG. 6. (Color online) Time response spectra of without HfO$_2$ inserted layer prepared with Au/Ni interdigitated fingers (inset) and with HfO$_2$ inserted MSM UV PDS fabricated with Ni and Au/Ni interdigitated fingers.

[1]D. Walker, A. Saxter, P. Kung, X. Zhang, M. Hamilton, J. Diaz, and M. Razeghi, Appl. Phys. Lett. 72, 3303 (1998).
[2]G. Hellings, J. John, A. Lorenz, P. Malinowski, and R. Mertens, IEEE Trans. Electron Devices 56, 2833 (2009).
[3]M. Asif Khan, M. Shatalov, H. P. Maruska, H. M. Wang, and E. Kuokstis, Jpn. J. Appl. Phys., Part 1 44, 7191 (2005).
[4]B. W. Lim, Q. C. Chen, J. Y. Yang, and M. Asif Khan, Appl. Phys. Lett. 68, 3761 (1996).
[5]Q. Chen, J. W. Yang, A. Osinsky, S. Gangopadhyay, B. Lim, and M. Z. Anwar, Appl. Phys. Lett. 70, 2277 (1997).
[6]R. Hickman et al., Solid-State Electron. 44, 377 (2000).
[7]Y. Kang, Y. Xu, D. Zhao, and J. Fang, Solid-State Electron. 49, 1135 (2005).
[8]D. Yoo, J. Limb, J.-H. Ryou, Y. Zhang, S.-C. Shen, R. D. Dupuis, D. Hanser, E. Preble, and K. Evans, IEEE Photonics Technol. Lett. 19, 1313 (2007).
[9]P. C. Chang, C. H. Chen, S. J. Chang, Y. K. Su, C. L. Yu, B. R. Huang, and P. C. Chen, Thin Solid Films 498, 133 (2006).
[10]P. E. Malinowski et al., Appl. Phys. Lett. 98, 141104 (2011).
[11]K. H. Chang, J. K. Sheu, M. L. Lee, S. J. Tu, C. C. Yang, H. S. Kuo, J. H. Yang, and W. C. Lai, Appl. Phys. Lett. 97, 013502 (2010).
[12]L. Sang, M. Liao, Y. Koide, and M. Sumiya, Appl. Phys. Lett. 98, 103502 (2011).
[13]M. L. Lee, T. S. Mue, F. W. Huang, J. H. Yang, and J. K. Sheu, Opt. Express 19, 12658 (2011).
[14]C. H. Chen, Y. H. Tsai, S. Y. Tsai, and C. F. Cheng, Jpn. J. Appl. Phys., Part 1 50, 04DG19 (2011).
[15]Y. Z. Chiou, J. Electrochem. Soc. 152, G639 (2005).
[16]C. J. Lee, Y. J. Kwon, C. H. Won, J. H. Lee, and S. H. Hahma, Appl. Phys. Lett. 103, 111110 (2013).
[17]C. H. Chen, Jpn. J. Appl. Phys., Part 1 52, 08JF08 (2013).

[18]X. Sun, D. Li, H. Jiang, Z. Li, H. Song, Y. Chen, and G. Miao, Appl. Phys. Lett. **98**, 121117 (2011).

[19]D. Derkacs, W. V. Chen, P. M. Matheu, S. H. Lim, P. K. L. Yu, and E. T. Yu, Appl. Phys. Lett. **93**, 091107 (2008).

[20]D. J. Chen, B. Liu, H. Lu, Z. L. Xie, R. Zhang, and Y. D. Zheng, IEEE Electron Device Lett. **30**, 605 (2009).

[21]Z. Q. Shi and W. A. Anderson, Solid-State Electron. **34**, 285 (1991).

[22]M. Liao, X. Wang, T. Teraji, S. Koizumi, and Y. Koide, Phys. Rev. B **81**, 033304 (2010).

[23]F. Zhang *et al.*, IEEE Electron Device Lett. **32**, 1722 (2011).

[24]L. Leung, A. F. Wright, and E. B. Stechel, Appl. Phys. Lett. **74**, 2495 (1999).

[25]M. M. Fan, K. W. Liu, Z. Z. Zhang, B. H. Li, X. Chen, D. X. Zhao, C. X. Shan, and D. Z. Shen, Appl. Phys. Lett. **105**, 011117 (2014).